Global Change Biology

Global Change Biology (2011) **17**, 886–897, doi: 10.1111/j.1365-2486.2010.02281.x

Evidence of increased net ecosystem productivity associated with a longer vegetated season in a deciduous forest in south-central Indiana, USA

DANILO DRAGONI*, HANS PETER SCHMID†, CRAIG A. WAYSON‡, HENRY POTTER§, C. SUSAN B. GRIMMOND¶ and JAMES C. RANDOLPH‖

*Department of Geography, Indiana University, Bloomington, IN, USA, †Atmospheric Environmental Research, Karlsruhe Institute for Technology (KIT/IMK-IFU), Garmisch-Partenkirchen, Germany, ‡USDA Forest Service, Newtown Square, PA, USA, §Rosenstiel School of Marine and Atmospheric Science, University of Miami, Miami, FL, USA, ¶Department of Geography, King's College London, London, United Kingdom, ‖School of Public and Environmental Affairs, Indiana University, Bloomington, IN, USA

Abstract

Observations of net ecosystem exchange (NEE) of carbon and its biophysical drivers have been collected at the AmeriFlux site in the Morgan-Monroe State Forest (MMSF) in Indiana, USA since 1998. Thus, this is one of the few deciduous forest sites in the world, where a decadal analysis on net ecosystem productivity (NEP) trends is possible. Despite the large interannual variability in NEP, the observations show a significant increase in forest productivity over the past 10 years (by an annual increment of about $10\,g\,C\,m^{-2}\,yr^{-1}$). There is evidence that this trend can be explained by longer vegetative seasons, caused by extension of the vegetative activity in the fall. Both phenological and flux observations indicate that the vegetative season extended later in the fall with an increase in length of about $3\,days\,yr^{-1}$ for the past 10 years. However, these changes are responsible for only 50% of the total annual gain in forest productivity in the past decade. A negative trend in air and soil temperature during the winter months may explain an equivalent increase in NEP through a decrease in ecosystem respiration.

Keywords: carbon cycle, climate change, eddy-covariance, leaf senescence, phenology

Received 6 April 2010; revised version received 28 May 2010 and accepted 9 June 2010

Introduction

Predicting the future roles of temperate forests in offsetting anthropogenic carbon emission requires an increase in our understanding of the mechanisms, controls, and feedbacks that regulate the interaction between the carbon cycle and climate variability and the future trends in carbon exchange between the ecosystem and the atmosphere (e.g., Schimel *et al*., 2001; Luyssaert *et al*., 2008).

The relation between climate, phenology, and the carbon cycle in temperate forests has been extensively documented (e.g., Keeling *et al*., 1996; Menzel & Fabian, 1999; Black *et al*., 2000; Chmielewski & Rotzer, 2001; Menzel, 2002; Estrella & Menzel, 2006; Delpierre *et al*., 2009; Penuelas *et al*., 2009). In general, a positive correlation between length of the vegetative season (V_{LENGTH}) and rise in average air temperature has been reported for several forest ecosystems across latitudinal and climatic gradients (e.g., Stöckli & Vidale, 2004; Linderholm, 2006; Menzel *et al*., 2006; Piao *et al*., 2007; Vitasse *et al*., 2009; White *et al*., 2009; Hu *et al*., 2010; Yanling *et al*., 2010). Forest productivity and carbon sequestration rates have been observed to be strongly linked with both air temperature and phenology (Goulden *et al*., 1996; Myneni *et al*., 1997; Valentini *et al*., 2000; Baldocchi *et al*., 2001, 2005; Cramer *et al*., 2001; Falge *et al*., 2002; White & Nemani, 2003; Churkina *et al*., 2005; Piao *et al*., 2008; Richardson *et al*., 2009; Yuan *et al*., 2009). Annual net ecosystem productivity (NEP) has been observed to increase as the net carbon uptake season becomes longer as a result of the rise in average temperatures (Myneni *et al*., 1997; Black *et al*., 2000; Baldocchi *et al*., 2005; Piao *et al*., 2007; Richardson *et al*., 2009; Yuan *et al*., 2009), but also there have been reports indicating that longer net carbon uptake seasons may correlate with decrease in annual NEP (Piao *et al*., 2008; Hu *et al*., 2010). However, the relation between variability in phenology and the forest carbon cycle is still unclear. While it is generally accepted that spring phenology is a strong determinant of productivity in deciduous forests (e.g., Botta *et al*., 2000; Richardson *et al*., 2006, 2009; Piao *et al*., 2008), there are also

Correspondence: D. Dragoni, Multi Science Building II, #310, 702 North Walnut Grove, Indiana University, Bloomington, IN 47405, USA, tel. +1 812 855 557, fax +1 812 855 1661, e-mail: ddragoni@indiana.edu

indications that the timing of senescence may play an important role in determining the annual NEP (Botta *et al*., 2000; Stöckli & Vidale, 2004; Piao *et al*., 2007). In particular, it is unclear to what extent the gain in gross ecosystem productivity (GEP), due to longer vegetative seasons, may be offset by concurrent increases in ecosystem respiration (R_e), due to higher temperatures (Goulden *et al*., 1996; Valentini *et al*., 2000; White & Nemani, 2003; Piao *et al*., 2008; Richardson *et al*., 2009). Because a temperature induced increase of summertime R_e would likely be due mostly to heterotrophic respiration (R_h), a multiyear trend could only be sustained by either shifting carbon pool sizes, or by a temporal shift of R_h from winter to summer. It is reasonable to assume that factors like composition, structure, age, and location of the forest may determine the sensitivity of the carbon cycle and phenology to climate variability (e.g., Richardson *et al*., 2009; Yuan *et al*., 2009). The magnitude of the ecosystem response may depend more on the relation between intraannual patterns of climatic variability and phenological cycle, rather than on trends in annual mean climatic conditions (e.g., Goulden *et al*., 1996; Schmid *et al*., 2000; Hu *et al*., 2010). For these reasons, investigating the dynamics between the carbon cycle and climate variability requires observational systems that operate at subannual temporal scale (e.g., daily to monthly) and long-term records (e.g., decadal or longer), which became available only recently (e.g., Wofsy *et al*., 1993; Schmid *et al*., 2000; Baldocchi *et al*., 2001; Richardson *et al*., 2009).

At the AmeriFlux site in Morgan-Monroe State Forest (MMSF) in south-central Indiana (USA), observations of carbon dynamics and climate have been taken since 1998 (Schmid *et al*., 2000; Baldocchi *et al*., 2001; Dragoni *et al*., 2007). In the course of a recent analysis of long-term variability in the MMSF carbon fluxes (Dragoni *et al*., 2007), a significant trend in annual NEP of about $10\,g\,C\,m^2\,yr^{-1}$ could be detected (Fig. 1). Here, we hypothesize that this increase in net productivity is the result of climatic trends affecting both the phenology and the carbon exchange processes in the forest ecosystem. The main objectives are to demonstrate that at the MMSF: (a) changes in forest phenology and carbon cycling are associated with climatic trends at the decadal (or longer) scale; (b) the phenological cycle has changed consistently with the NEP trend observed during the past 10 years; and (c) the response of carbon dynamics to climate variability is dependent on phenology.

Materials and methods

Study site

The MMSF in Indiana (USA, 39°19′N, 86°25′W) is a secondary successional broadleaf forest with 29 identified species in the immediate vicinity of an eddy-covariance tower (Schmid *et al*., 2000; Ehman *et al*., 2002), about 75% of which are sugar maple (*Acer saccharum*), tulip poplar (*Liriodendron tulipifera*), sassafras (*Sassafras albidum*), white oak (*Quercus alba*), and black oak (*Quercus nigra*). Average canopy height is about 27 m, and mean age of the trees is 80–90 years. The area has ridge/ravine topography with a relative relief of <60 m, and an overall drop of 90 m in 4 km (Schmid *et al*., 2000); average elevation is about 275 m a.s.l. Soils in the area are mesic Typic Dystrochrepts dominated by the Berks–Weikert complex, defined as moderately deep and shallow (0.5–1.5 m in the tower area), steep and very steep, well drained silt-loam formed in residuum from sandstone, siltstone, and shale (Wayson *et al*., 2006).

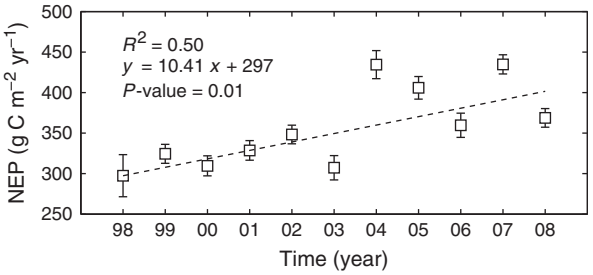

Fig. 1 Annual net ecosystem productivity (NEP) at the Morgan-Monroe State Forest (MMSF) as estimated from eddy-covariance measurements. Error bars describe the random uncertainty on the estimates (Dragoni *et al*., 2007). Because measurements at MMSF started in spring 1998, the ecosystem respiration for the first part of the year was estimated using winter respiration observations from the successive years (Schmid *et al*., 2000). Observations from 1998 were excluded from any further trend analysis.

Eddy-covariance measurements

Since early spring 1998, eddy-covariance observations have been taken from the top of the 46 m tower. Carbon dioxide fluxes (F_C) are measured using a three-dimensional sonic anemometer (CSAT-3, Campbell Scientific Inc., Logan, UT, USA) and a closed-path infrared gas analyzer (IRGA, LI-6262, LI-COR Biosciences, Lincoln, NE, USA; LI-7000 after 2004). The sampled air is pulled from the sonic level to the IRGA located in the shelter at the bottom of the tower. Data acquisition frequency is 10 Hz. Postprocessing expresses mixing ratios relative to dry air (equivalent to the so-called WPL correction, e.g., Leuning, 2004), and accounts for spike detection and removal, the time lag between gas concentration data and vertical wind velocity measurements, velocity vector rotation to hourly streamline coordinates, and eddy-covariance fluxes are calculated as hourly averages. The F_C values are subject to quality control (including outlier rejection, and a friction velocity criterion, i.e., $u^* \leq 0.3\,m\,s^{-1}$ to reject values obtained under low turbulence conditions, where the change of CO_2 storage in the canopy air space could be important). Further details are described in Schmid *et al*. (2000). Values of F_C that passed the quality control criteria are considered acceptable as

estimates of net ecosystem exchange (NEE = −NEP) and used to calculate annual NEP. Given the difference in technology between the two IRGA models, a direct *in situ* comparison between the two was performed by connecting a LI-6262 in series with the LI-7000 of the MMSF system, using the same sample line and associated with the same sonic anemometer (CSAT-3). This in series configuration (LI-7000 before LI-6262) was run for 1 week and then in reverse order for another week. The results of the two models were indistinguishable.

Rejection of measured flux values during quality control creates data gaps that need to be filled before calculation of the annual total NEP. To fill hourly NEE time series gaps, simple parametric models are applied that link soil temperature (T_S) to ecosystem respiration [$R_E = a_1 \exp(a_2 T_s)$], and photosynthetic photon flux density (PPFD) to GEP [$= (a_3 \text{PPFD})/(a_4 + \text{PPFD})$], as described in Schmid *et al*. (2000, 2003), such that NEE = GEP − R_E. The free parameters a_3 and a_4 for the GEP estimate are derived by nonlinear regression, based on data that meets the quality control criteria for 10-day block periods of the vegetative season during each year, whereas parameters a_1 and a_2 to estimate R_E are determined annually. Uncertainty on flux estimates was estimated according to Dragoni *et al*. (2007), based on the work of Hollinger & Richardson (2005).

Environmental and climate observations

Measurements of PPFD (Li-190SA-50, LI-COR Biosciences and BF3, Delta-T Devices Ltd., Cambridge, UK since 2007), air temperature (HMP35C, Vaisala, Helsinki, Finland, and VTP37, Meteolabor AG, Wetzikon, Switzerland, since 2006), and precipitation (Texas Electronics, Dallas, TX, USA) used in this work were obtained from the instrumentation located at the top of the eddy-covariance tower. Soil temperature at a depth of 5 cm and volumetric water content (VWC) for the first 30 cm are regularly measured using thermocouples (TCAV, Campbell Scientific Inc.) and time domain reflectometer (TDR, CS615 and CS616, Campbell Scientific Inc.) located at four different locations inside the footprint of the eddy-covariance tower. TDR measurements are corrected for soil temperature and for the specific type of soil by using coefficients determined from weekly gravimetric samples and corresponding measurements of the TDR probes. The averages from all four locations were used in our analysis.

Temperature exerts a strong control on physiological processes like leaf senescence. However, rather than absolute values of temperature, the sum of the degrees below a specific threshold (cold degree-days, in °C) are used (e.g., Dufrene *et al*., 2005). The total cold degree-days from day of the year (DOY) 140 to 290 (i.e. the period with fully developed green canopy) were calculated by summing the deviation of daily mean air temperature at 46 m from a threshold temperature of 21 °C (10-year mean air temperature for the same seasonal period).

Phenology parameters

Start, end, and length of the vegetative season (V_{START}, V_{END}, and V_{LENGTH}, respectively) and net carbon uptake season (C_{START}, C_{END}, and C_{LENGTH}, respectively) were estimated using different independent approaches to overcome specific limitations associated with each method and reduce the uncertainty in the results. The approaches monitor different processes within the ecosystem (e.g., leaf development, NEE of carbon). Therefore, the derived phenological parameters and their respective trends are not exactly congruent (e.g., White & Nemani, 2003; Piao *et al*., 2008). Nevertheless, these parameters are the net results from the same temporal patterns within this forest and should be temporally consistent relative to each other.

Vegetative season

In this work, the start, end, and length of the vegetative season were identified using two indirect methods based on: (a) ground-based observations of vegetation area index (hereafter, VAI-2000); (b) digital photography (hereafter greenness index).

VAI-2000

VAI observations have been collected regularly since early 1999 along three radial transects (10 points each, 15 m apart) extending from the eddy-covariance tower towards the south-west, west, and north-west cardinal directions (i.e., inside the main foot-print of the eddy-covariance tower). Measurements with a LAI-2000 system (LI-COR Biosciences; observations at 1.8 m aboveground and above canopy reference) have been taken weekly during spring and fall, and biweekly during the central part of the summer. In the fall, observations have continued until no nominal change in VAI remained and resumed right before bud break. The TIMESAT software (Jonsson & Eklundh, 2002, 2004) was run using MATLAB (version 2009b, Mathworks Inc., Natick, MA, USA) to determine phenological parameters. TIMESAT is a software package for investigating seasonality in time-series data and their relation with dynamic properties of vegetation, such as phenology. A 20% VAI threshold was arbitrarily selected to determine the start, the end, and the length of the vegetative season (V^{VAI}_{START}, V^{VAI}_{END}, and V^{VAI}_{LENGTH}, respectively). The TIMESAT algorithm, while robust to sparse gaps, requires nearly continuous time-series data. Hence, the LAI data were filled for the winter months using a simple linear interpolation between points to obtain the data series suitable for analysis. As MMSF is a deciduous forest, it is assumed that this interpolation in winter did not affect the phenology outputs used in our analysis as the winter values are used as a baseline for the LAI amplitude output. Annual V^{VAI}_{START}, V^{VAI}_{END}, and V^{VAI}_{LENGTH} were determined based on the mean values from all 30 observations from the three transects. The spatial standard deviation was used as a measure of uncertainty in the phenology parameters.

Greenness index

Digital photographs taken from the top of the eddy-covariance tower were used to determine the presence of green leaves in the forest canopy. Pictures were taken weekly towards the four cardinal directions. Images were manually edited to remove

sky pixels and nonforest canopy objects (such as tower instrumentation). As pictures were taken manually with different cameras, their quality varied considerably over the 10 years of observations (1999–2008). To ensure consistency, several objective criteria for quality control were adopted. Images were excluded which had too low resolution, were too bright or too dark [using the Hue, Saturation and Value decomposition (HSV) Crimmins & Crimmins, 2008], or images in which colors were clearly altered, like for instance by the direct canopy reflection of solar light during early or late hours in the day. As a result, the final data set included 1211 images from 2000 to 2008. Each pixel of a given image was decomposed in its red (R), blue (B), and green (G) components and the greenness index for each pixel (g_p) was calculated as the relative green brightness (Richardson *et al*., 2007)

$$g_p = \frac{G}{R + G + B}. \quad (1)$$

A single greenness for each image (g_i) was calculated as the average of all pixel indices g_p. The g_i for the four cardinal directions were used to determine the spatial mean time series of the greenness index. The spatial standard deviation of the four g_i values was used as a measure of the uncertainty in the estimates. In the RGB decomposition, the G component is present also in colors that are not necessarily tonalities of green (like yellow, orange, or brown) and green tonalities contain R and B components as well. For this reason, values were normalized using the winter and mid-summer baselines as constrains to obtain a range between 0 (no canopy greenness) and 1 (maximum canopy greenness). To determine the start, end, and length of the vegetative season (V_{START}^{GREEN}, V_{END}^{GREEN}, and V_{LENGTH}^{GREEN}, respectively), a sigmoid function was fitted to the 'greening-up' (i.e. DOY, <200) and the 'greening-down' (i.e. DOY >150) part of the year, using the standard deviation of each data point as a weighting factor. This ensures an accurate description of the greenness patterns in the early spring and late fall, rather than the mid-part of the vegetative season. The beginning of the season was determined as the point in the fit where mean g_i was for the first time larger than the root mean square error (RMSE) of the fit (i.e., when g_i became significantly different from zero). Identification of the end of the season was more difficult, because of the larger portion of G components in the residual foliage with 'fall colors'. It was determined as the last point in the fit where g_i was larger than 0.23 (average RMSE for the late-season fits is 0.13). This number was determined using the HSV decomposition of hourly images taken from an automatic fixed digital camera installed on the tower in late summer 2008. With the HSV decomposition, the absence of green pixels in the images is more clearly defined as 0, which correspond to a greenness index value of 0.23. To quantify the uncertainty on annual V_{START}^{GREEN}, V_{END}^{GREEN}, and V_{LENGTH}^{GREEN}, a Monte Carlo simulation was used to generate 10 000 synthetic time series of daily greenness indexes for each year. Each daily g_i value was generated from a normal distribution with mean and standard deviation equal to the values and the RMSE of the sigmoidal fit, respectively. For each of the 10 000 time series, the synthetic start, end, and length of the vegetative season were determined using the method described for the actual parameters. Uncertainties were defined as the standard deviations of all synthetic V_{START}^{GREEN}, V_{END}^{GREEN}, and V_{LENGTH}^{GREEN}.

Net carbon uptake season

The start, end, and length of net carbon uptake season (C_{START}, C_{END}, and C_{LENGTH}) were estimated for each year (1998–2008) using a 5-day moving average of daily total NEP. The start of the season was identified by the first day of the year when values in the time-series became positive, and the end of the season by the first day when the total daily NEP became negative again. The uncertainty in the eddy-covariance estimate of NEP directly propagates to the daily total NEP and therefore to the estimates of the start and the end of the net carbon uptake seasons. In order to quantify the uncertainty on C_{START}, C_{END}, and C_{LENGTH}, a Monte Carlo simulation was used to generate 10 000 synthetic time series of hourly NEP for each year. Hourly values of NEP were generated from a double-exponential distribution with mean and standard deviation equal to the actual measured NEP and the estimated random uncertainty, respectively (Dragoni *et al*., 2007). Hourly synthetic NEP was aggregated to daily time scales, obtaining 10 000 daily time series for each year. The synthetic C_{START}, C_{END}, and C_{LENGTH} were calculated using the 5-day moving average, as described above, and the annual uncertainty in each parameter was calculated as the standard deviation of the synthetic C_{START}, C_{END}, and C_{LENGTH}.

Trend analyses

Linear regressions (weighted by the inverse of the squared error) with time were performed to identify trends in phenology at the MMSF. A trend was determined to be significant if the slope of the linear regression was different from zero with a 95% interval of confidence. For all the parameters obtained using LAI-2000, and the greenness-index approaches, the error was assumed to be normally distributed, and the sum of the squared differences between measured and modeled values was adopted as a merit function (Press *et al*., 2002). However, the errors in the net carbon uptake season parameters followed more closely a double-exponential distribution and thus the sum of the absolute difference between measured and modeled values was used as a appropriate merit function (Press *et al*., 2002; Willmott *et al*., 2009). Daily totals of NEP, GEP, R_e, PPFD, precipitation, and daily averages of ecosystem light-use efficiency (LUE = GEP/PPFD), air and soil temperature, and VWC were used to investigate for temporal trends in the 10-year long data set (i.e. 1999–2008, 1998 was excluded from the trend analysis because measurements were not taken in the earliest part of the year). Moving block averages over 30 days from each year were regressed with time, defined as the number of years after 1999. The 30-day box-car window was chosen as a compromise between increasing the statistical significance of the regression analysis over the large interannual variability and resolving the intraannual patterns of carbon fluxes and its drivers. The slope of the fits and its 95% confidence interval were used to detect the presence of trends during any part of the calendar year.

Results

The start of the vegetative and carbon seasons ranged from DOY 105 to 118 (Table 1). As expected, C_{START} follows V_{START}, but with some differences among methods. V_{START}^{GREEN} is the earliest (DOY 105), while V_{START}^{VAI} is DOY 116 on average. The average C_{START} is about 13 days after V_{START}^{GREEN}, but only 2 days after V_{START}^{VAI}. The early date of V_{START}^{GREEN}, derived from images taken at an oblique angle, reflects the change in greenness induced by the early development of the understory vegetation, whose carbon assimilation is not large enough to move the ecosystem from carbon source to sink. In contrast, the understory foliage (below the VAI observation height, 1.8 m) has no bearing on V_{START}^{VAI}. Thus, V_{START}^{VAI} responds primarily to the development of tree leaves and consequently occurs closer to C_{START} (Table 1). The standard deviation of the season start over the analyzed years is around 4 days in all methods, with the exception of V_{START}^{VAI} where it is 6 days (Table 1). Depending on the method, V_{END} ranges from DOY 292 to 322, while C_{END} is estimated to be DOY 287. V_{END}^{VAI} is after DOY 315 on average, a time of year when digital cameras images reveal the canopy to be at leaf-off or in late stages of senescence. The V_{END}^{VAI} estimates are later because senesced leaves continue to be measured until they fall from the tree. C_{END} (DOY 287) precedes V_{END}^{GREEN} method by 5 days (Table 1). The average length of the season ranges between 170 (C_{LENGTH}) and 206 days (V_{LENGTH}^{GREEN}) with interannual standard deviation between 9 and 13 days (Table 1). The differences in the season start, end, and length estimators between methods is larger than the interannual variations, which indicates that each method reflects a systematic, but different, response to the complex and multifaceted seasonal phenology development.

The result of the decadal trend analysis of phenology season estimators is consistent between methods. There is no significant change in V_{START} (Table 1, Fig. 2). C_{START} has a weak (<1 day later per year) positive trend. It is significant at the 95% confidence interval, but is likely dominated by the last 2 years (2007 and 2008). V_{END} and C_{END} exhibit strong significant trends (Table 1, Fig. 2), which range from 2.6 (V_{END}^{VAI}) to 3.1 days yr^{-1} (V_{END}^{GREEN}). Very similar results are obtained for V_{LENGTH}, which increased by 3.3 and 2.6 days yr^{-1} (V_{LENGTH}^{GREEN} and V_{LENGTH}^{VAI}, respectively), and C_{LENGTH}, which increased by 2.3 days yr^{-1}. Thus, the average observed trends of these phenology estimators suggests that the vegetative season at MMSF has increased by 30 days over the past 10 years, with the senescence period moving from early to late October.

A strong correlation exists between V_{LENGTH}^{GREEN}, C_{LENGTH} and the annual NEP (P-value <0.05 and $R^2 > 0.6$, Fig. 3). The corresponding increment of NEP is 5–7 g C m^{-2} for each additional day in the vegetative or net carbon uptake season. The correlation between the annual NEP and V_{LENGTH}^{VAI} is weaker and not significant (not shown).

The analysis of the seasonal distribution of daily total NEP shows a substantial positive trend over the 10-year period at the end of the summer, between DOY 260 and 300 (Fig. 4a). During this time of year, the change in NEP is on average 0.1 g C m^{-2} day^{-1} yr^{-1}, with a peak change of about 0.2 g C m^{-2} day^{-1} yr^{-1} between DOY 280 and 300. A positive trend occurs also in GEP during the same period and, to a lesser extent and slightly earlier, in R_e (Fig. 4b and c). The NEP trend between DOY 260 and 300 leads to a change in the annual NEP of 40–50 g C m^{-2} over 10 years (Fig. 5a), or about 15% of the average annual NEP. This increase in forest productivity, however, can explain only about 40–50% of the trend in annual NEP observed at the MMSF (Fig. 1). A small, but significant negative trend is noticeable during the winter months in both NEP and R_e (Fig. 4a and b). This trend is only about -0.03 g C m^{-2} day^{-1} yr^{-1}, but it is consistent from November until most of March and contributes to the overall

Table 1 Phenology parameters and corresponding trends as estimated using the three different methods: VAI-2000, greenness-index and eddy-covariance

	Season parameters			Trends (days yr^{-1})		
Method	Start (DOY)	End (DOY)	Length (days)	Start	End	Length
VAI-2000 ($V_{START, END, LENGTH}^{VAI}$)	116.4 (6.2)	322.4 (13.8)	206.0 (13.4)	−0.8 (0.12)	2.6 (0.02)	2.6 (<0.01)
Greenness-index ($V_{START, END, LENGTH}^{GREEN}$)	104.9 (4.1)	292.3 (9.8)	187.4 (10.7)	−0.4 (0.51)	3.1 (<0.01)	3.3 (<0.01)
Eddy-covariance ($C_{START, END, LENGTH}$)	118.2 (3.9)	287.0 (9.4)	170 (8.7)	0.9 (<0.01)	3.0 (<0.01)	2.3 (<0.01)

The start, end (day of the year, DOY) and length (days) of the vegetative (V_{START}, V_{END}, and V_{LENGTH}, respectively) and net carbon uptake (C_{START}, C_{END}, and C_{LENGTH}, respectively) seasons are the averages from all the observation years (with standard deviation). Trends for the start, end, and length of the season were estimated using weighted linear regressions. The resulting slopes (and their P-values) are reported as the gain (positive) or loss (negative) of days per year.
VAI, vegetation area index.

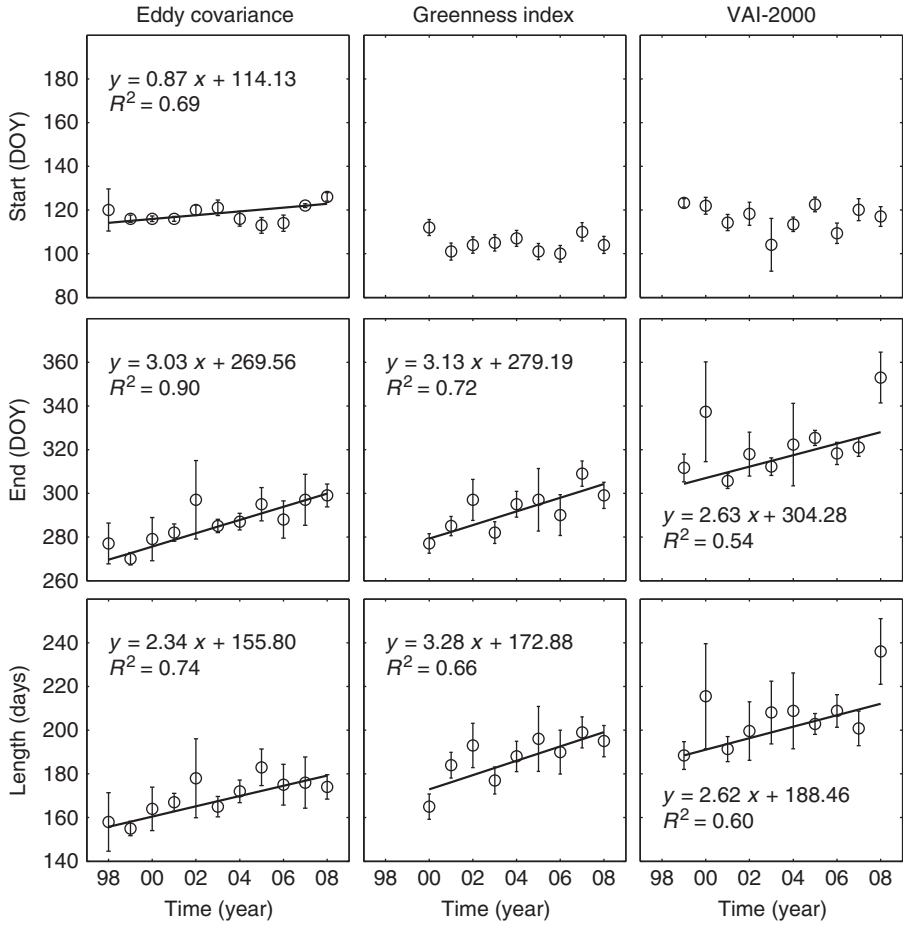

Fig. 2 Start, end, and length of the vegetative and net carbon uptake seasons by year as estimated using vegetation area index (VAI-20000, greenness index, and eddy-covariance approaches. The weighted linear fits are shown when significantly different from 0 with a 95% confidence interval.

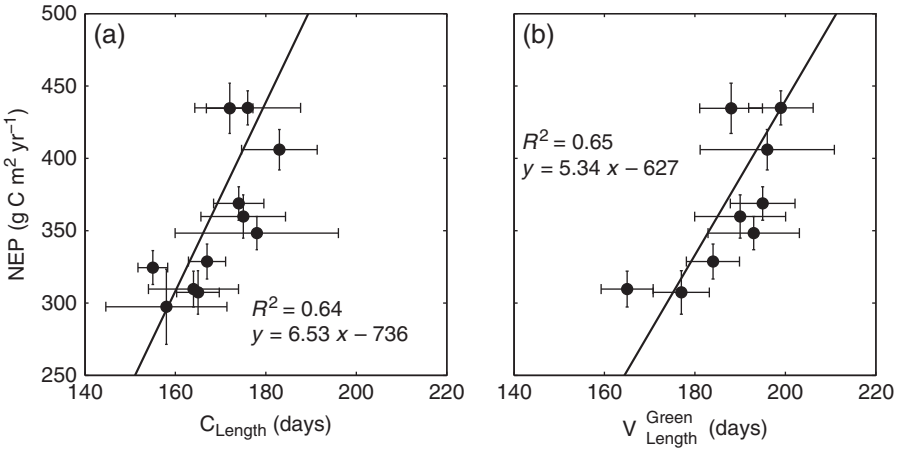

Fig. 3 Weighted total least squares regression analysis between annual net ecosystem productivity (NEP) and (a) length of the net carbon uptake season (C_{LENGTH}); (b) length of the vegetative season from the greenness-index method (V^{GREEN}_{LENGTH}). Solid lines describe the weighted total least square fits. Error bars represent the NEP uncertainty estimated using Dragoni *et al*. (2007).

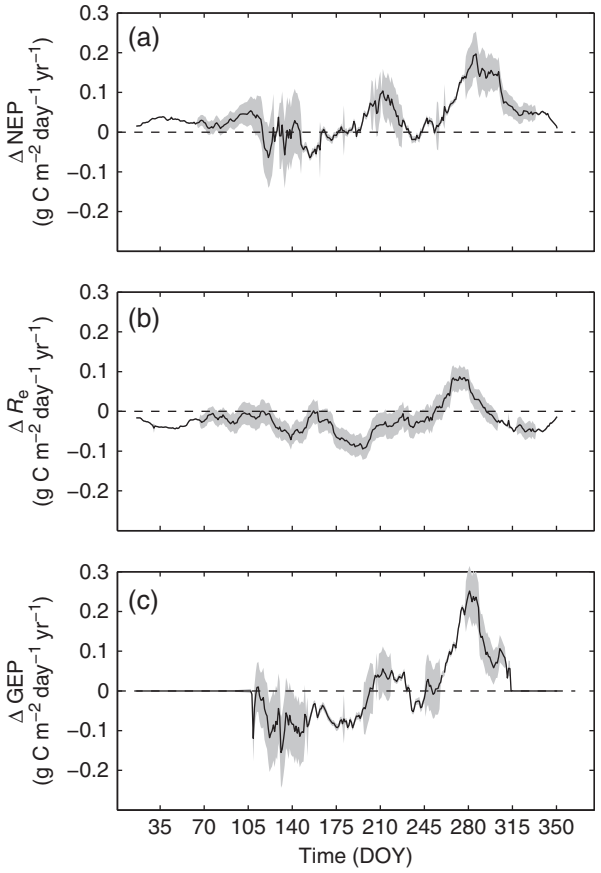

Fig. 4 Slopes (solid line) of the running 30-day interval data regressed against time (10 years) of (a) daily total net ecosystem productivity (NEP), (b) ecosystem respiration (R_e), and (c) gross ecosystem productivity (GEP). Gray areas represent the 95% confidence interval for the slope.

reduction in annual respiration (and therefore increase in NEP) of about 30–40 g C m^{-2} in 10 years (Fig. 5b). Remarkably, this amount seems to explain most of the remaining total increase in net annual productivity at the MMSF since 1998 (i.e. about 110 g C m^{-2}, Fig. 1). A few other significant trend periods can be identified in R_e and GEP during the central part of the vegetative season (for instance, between DOY 170 and 200). However, because these trends mostly constitute mutually off-setting reductions in GEP and R_e, the net result amounts to very little change in NEP. One should note that the partitioning of NEP into R_e and GEP depends on the parametric model for R_e (see earlier section on Eddy-covariance measurements). Thus, the relative magnitudes of trends in R_e and GEP may be affected by the model and should be interpreted with care.

The analysis of daily average air temperature indicates that there is no significant decadal trend in either average annual temperature (P-value >0.6, not shown) or average temperature during the vegetative season (P-value >0.2, not shown). However, the same analysis shows four shorter periods of subseasonal length that exhibit significant decadal trends (Fig. 6a). Two periods with negative trends of about $-0.5\,^{\circ}$C day^{-1} yr^{-1} can be observed during the winter, from DOY 40 to 70 (February) and from DOY 320 to 350 (November–December). Two positive trend periods are identified between DOY 160 and 200 (June–July), and between DOY 260 and 280 (September–October). Both summer trend periods suggest a rise in temperature of about 0.3–0.4 $^{\circ}$C day^{-1} yr^{-1}. Daily total precipitation and PPFD do not have significant decadal trends (not shown). Soil temperature, as expected, approximately follows air temperature with a significant negative

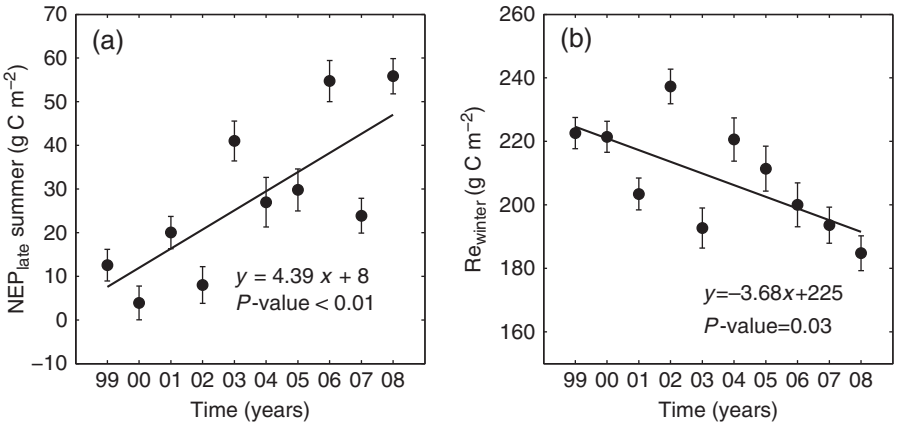

Fig. 5 (a) Total net ecosystem productivity in late summer (NEP_{ls}) and (b) ecosystem respiration in late-fall and winter ($R_{e_{fw}}$) from 1999 to 2008. NEP_{ls} is the total NEP from day of the year (DOY) 260 to 299. $R_{e_{fw}}$ is the total respiration from DOY 300 of the previous year to 90 of the specific year. Error bars are the uncertainties on $R_{e_{fw}}$ and NEP_{ls} estimated using Dragoni *et al*. (2007). Solid lines are the weighted total least square fits.

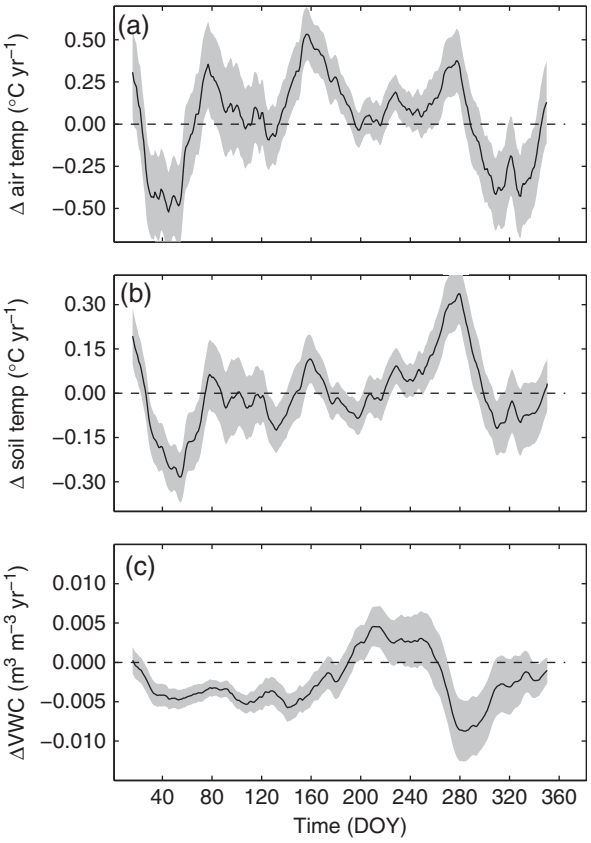

Fig. 6 Ten-year trends in daily averages of (a) air temperature at 46 m (Air Temp), (b) soil temperature (5 cm depth, Soil Temp), and (c) soil volumetric water content in the first 30 cm of depth (VWC). Trends were calculated regressing 30-day data moving blocks with time. Solid lines describe the slope of the linear regression of daily totals/averages vs. time, and gray areas represent the 95% confidence interval for the slope.

decadal trend peaking at $-0.3\,^{\circ}\mathrm{C\,day^{-1}\,yr^{-1}}$ during the month of February, and a positive trend peaking at $0.3\,^{\circ}\mathrm{C\,day^{-1}\,yr^{-1}}$ between DOY 260 and 280 (Fig. 6b). The daily average of the VWC shows a small negative decadal trend (drying) for most of the year except for a period with a weak wettening trend in summer (mid-July to mid-September, Fig. 6c).

Further indication of how long-term trends may affect ecosystem processes is found in the variability of the absolute values of climatic and environmental variables. The negative trend in air temperature recorded during February (Fig. 6a) indicates daily averages approaching the freezing point (Fig. 7a). The positive trend at the end of the summer is associated with daily averages that have increased from about 15 to 20 °C (Fig. 7b) and similarly for soil temperature (Fig. 7c and d). In 2008, the daily mean soil temperature was below 0 °C for the first time in 10 years. The negative trend in VWC during most of the first part of the year (Fig. 6c) may be irrelevant in terms of plant physiology. The amount of water in the first 30 cm of soil declines only from 0.45 to about $0.40\,\mathrm{m^3\,m^{-3}}$ (Fig. 7e), still enough to support the transpiration demand by trees (later in the season). However, the decline during the end of the summer (Fig. 6c) may cause the VWC to fall below $0.2\,\mathrm{m^3\,m^{-3}}$ (Fig. 7f), which may induce water stress in some of the species found at the MMSF (Dragoni *et al*., 2009).

Total cold degree-days from DOY 140 to 290 range between 100 and 400 °C and show a significant negative trend of about $-25\,^{\circ}\mathrm{C\,yr^{-1}}$ from 1999 to 2008 ($R^2 = 0.58$ and P-value = 0.01, Fig. 8a). This change reflects the warming trends observed in air temperature during the first and last part of the vegetative season (Fig. 6a). Remarkably, total cold degree-days show a strong and significant correlation with $V_{\mathrm{END}}^{\mathrm{GREEN}}$ ($R^2 = 0.93$ and P-value < 0.01, Fig. 8b), confirming that the rate at which senescence occurs is highly correlated with, and perhaps governed by, air temperature.

Discussion

Our results present strong evidence for a change in phenology and carbon cycling at the MMSF, seemingly driven by decadal trends in air and soil temperature. Two independent phenological estimators suggest that no significant changes are occurring at the start of the growing season/spring (Fig. 2). The start of the net carbon uptake season exhibits an overall positive (later) but very weak trend ($< 1\,\mathrm{day\,yr^{-1}}$) that is likely due to two unusual years at the end of the observed decade. However, there are no other results in our analysis supporting this tendency, with NEP even showing a positive trend during the early part of spring (Fig. 4a). All the methods used to estimate the end of the vegetative and net carbon uptake seasons show significant and very similar trends in V_{END} and C_{END}, with both extending by about $3\,\mathrm{days\,yr^{-1}}$. Trends in forest phenology have been reported by a number of previous studies. In an analysis of direct observations of plant phenology over Europe for the period 1971–2000, Menzel *et al*. (2006) found an average advancing trend of $0.25\,\mathrm{days\,yr^{-1}}$ (earlier) in spring onset. However, they did not find a clear result for the onset of senescence and noted that there were fewer records available for this phenology trait. Stöckli & Vidale (2004) determined a delay of senescence by an average of $0.42\,\mathrm{days\,yr^{-1}}$ over Europe (between 1982 and 2001), using normalized difference vegetation index (NDVI) from the NOAA/NASA Pathfinder NDVI data set. Piao *et al*.'s (2007) analysis (based on the ORCHIDEE global vegetation model, Botta *et al*., 2000) for the past 20 years found a

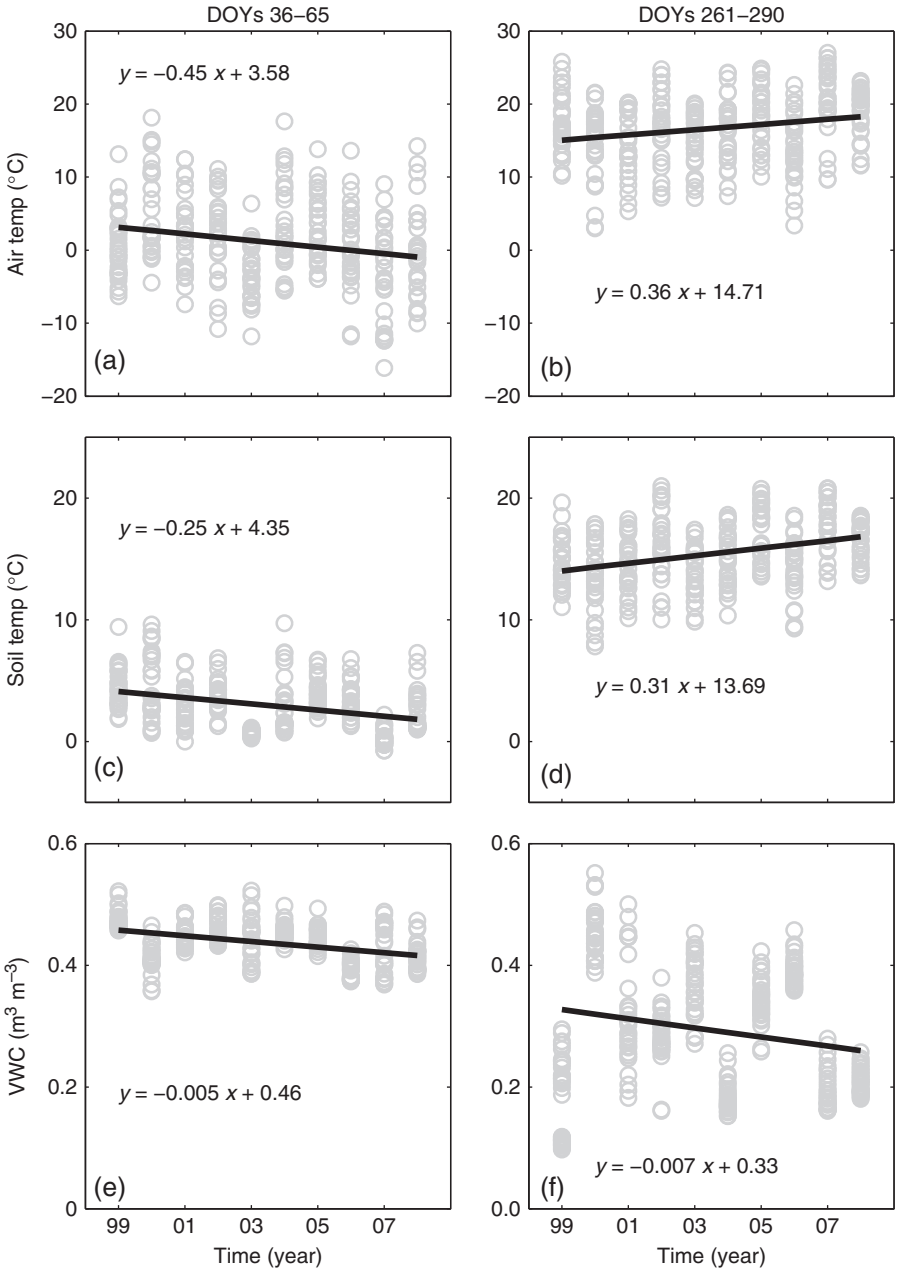

Fig. 7 Regression analysis between daily averages variables (single empty circles) and time for: (left) winter [day of the years (DOYs) 36–65], and (right) end of the summer (DOYs 261–290); for air temperature at 46 m (top), soil temperature at 5 cm (middle), and soil volumetric water content 0–30 cm (bottom). Regression equations are shown for each variables all the *P*-values for the slope coefficients are <0.01.

global lengthening of the vegetative season from both earlier spring and later senescence with a significant delay in the senescence by 0.5 days yr^{-1} in mid-to-high latitude ecosystems in North America. These trends are not as strong as those observed i*n situ* at MMSF. These all use satellite-derived data to either directly infer the phenological parameters (Stöckli & Vidale, 2004) or to develop and drive a vegetation model (Piao *et al*., 2007). In this respect, the discrepancy with the trend observed using other approaches (i.e. VAI-2000 and greenness index) might reflect limitations in detecting correctly the phenological traits (in particular the end of the vegetative season) with remote sensing technology (White *et al*., 1999). As Stöckli *et al*. (2008) noted, these limitations may be a consequence of interpolation errors of gaps in the time-series due to cloud cover (in

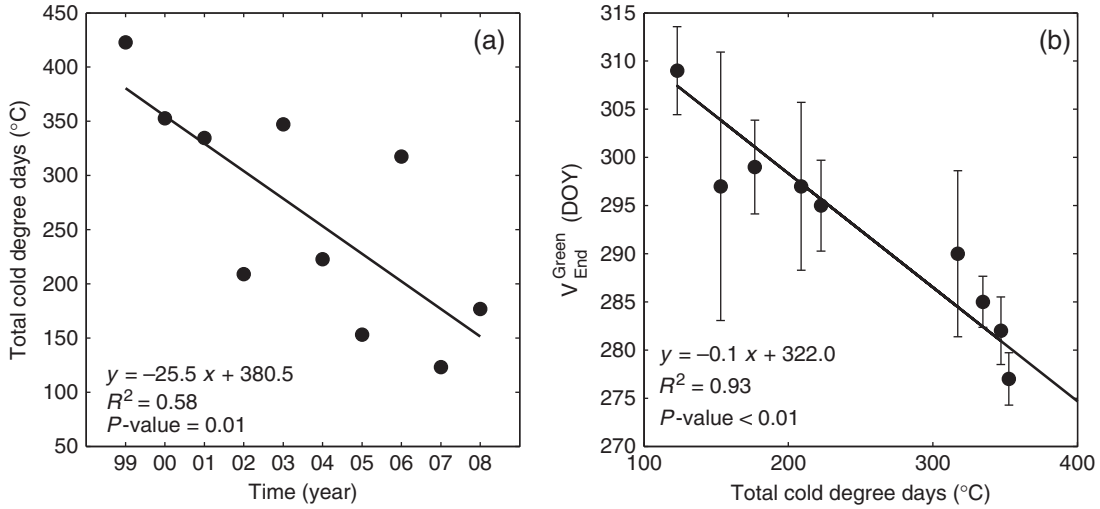

Fig. 8 (a) Total cold degree-days between day of the year (DOY) 140 and 290 from 1999 to 2008. Solid line is the total least square fit. The temperature threshold used to calculate the cold degree-days was 21 °C, which is the 10-year (1999–2008) average air temperature for the period between DOY 140 and 290. (b) End of the season estimated using the greenness-index (V_{END}^{GREEN}) as a function of the total cold degree-day. Error bars describe the uncertainty in the estimates of the end of the season. Solid line is the weighted total least square fit. Regression equation, regression coefficient, and *P*-value are reported for both fits.

particular during fall in many temperate regions), and, more generally, due to problems associated with spatial resolution and spatial parameter averaging.

Our results suggest that trends of rising air, soil temperatures, and decreasing cold degree-days during the summer (Figs 6a, b and 8) drives the positive trend in V_{END}. In fact, it is well recognized that air temperature exhibits a control on senescence, even though the mechanisms are not well understood (e.g., Menzel, 2002; Estrella & Menzel, 2006; Piao *et al*., 2007; Delpierre *et al*., 2009). The strong correlation between cold degree-days and V_{END}^{GREEN} (Fig. 8b) confirms the importance of cumulative heat deficit in determining the senescence rate, and therefore the length of the vegetative season. Moreover, our results show evidence of a significant declining trend in cold degree-days during the summer between 1999 and 2008 (Fig. 8a), indicating that decadal climatic trends may be responsible for the observed changes in senescence and phenology patterns at MMSF.

The observed link between decadal trends of growing season length and annual NEP at MMSF, finds analogous results in Baldocchi *et al*. (2001) and Baldocchi (2008), who report a strong correlation between annual NEP and growing-season length for 10 broad-leaf forest Fluxnet sites ranging across boreal to low temperate latitudes in North America (including MMSF), Europe and Japan. Similar results, based on modeling approaches supported by satellite data, are also found by Churkina *et al*. (2005), suggesting a very general and robust relation between growing season length and NEP that holds across a wide range of climatic and ecophysiological conditions. However, caution needs to be exercised when comparing interannual variability at a given site with variability across different sites (i.e. space-for-time studies), as uncertainty is introduced by the differences in ecosystem structure and functionality (e.g., Richardson *et al*., Philosophical Transactions of the Royal Society, in press).

Our results suggest that only about 50% of the annual trend in NEP can be attributed to the actual increase of V_{LENGTH} and C_{LENGTH}, while the other 50% is likely due to the reduction in respiration during the nonvegetative season. Thus, the actual change in NEP due to delay in senescence in is about $3\,g\,C\,m^{-2}\,day^{-1}$. This shows that in a deciduous forest like MMSF, the sensitivity of carbon cycle to climate variability is dependent not only on the sign and magnitude of the climate change, but also on its timing with respect to the phenological stages.

Piao *et al*. (2008) reported a substantial decrease in NEP in the northern hemisphere associated with higher temperatures in fall. Their results, based on observations of atmospheric CO_2 concentration patterns, eddy-covariance sites, and simulations with the ORCHIDEE model, indicate an overall reduction of the duration of the net carbon uptake season. Their analysis suggests that higher temperatures in fall are associated with longer vegetative seasons and higher assimilation rates, but also with a much larger increase in respiration causing lower NEP. Our results indicate that the increase in respiration caused by a longer vegetative season does not offset the increase in assimilation (Fig. 4b and c), with the opposite result that the carbon uptake season is becoming longer, not shorter (Fig. 2). This contradiction most likely

originates from the difference in spatial scales and forest types between the studies. In Piao *et al.*'s (2008) study 16 of the 25 eddy-covariance sites are in evergreen forests (their table S4 in the supporting information). This is an important difference to our work, considering the well-documented differences in respiration and assimilation sensitivities to environmental variability between the two different types of ecosystems (e.g., Falge *et al.*, 2002; Yuan *et al.*, 2009).

This work raises two important questions, how long can the trends observed at the MMSF continue? And, what are the allocation patterns for the carbon assimilated during the longer vegetative season? Answering these is beyond the scope of our work, but hypotheses can be suggested. The warming trend during part of the summer may continue, but as the vegetative season extends further into the fall, colder air and soil temperature will impose strong limitations to the phenology trend. This is particularly important in light of the observed negative trend of air temperature during the winter. Also, soil moisture may play a critical role, as the extended presence of an active canopy may further reduce soil water availability during a period when water can already be a limiting factor. Our regular measurements of tree diameter at breast height taken on numerous trees around the eddy-covariance tower (Ehman *et al.*, 2002) indicate that the growth of the aboveground woody biomass stops before late summer, suggesting that the carbon assimilated during the extended part of the vegetative season may not be directly allocated to this pool. Other allocation patterns can be suggested, including allocation as a labile carbon for the growth in the following years (e.g., Gough *et al.*, 2009), increased root production, or increased exudates as a mechanism to enhance nutrient availability by the rhizosphere microbes (e.g., Phillips *et al.*, 2009). However, there is a lack of evidence because of the short period (relative to the temporal scale of climatic change) of observations and partial understanding of the mechanisms, controls, and feedbacks that regulate deciduous forests' (or MMSFs) response to climate variability. For this reason, long-term observations of ecosystem processes are critical for monitoring and prediction of current and future role of deciduous forests in the global carbon cycle.

Conclusions

Our decadal observations of carbon exchange over a deciduous forest in south-central Indiana exhibit an increase in net carbon uptake over time. This increase in productivity is likely to be caused by observed changes in phenology and carbon cycling. In turn, these trends in phenology are likely attributable to decadal or longer-term climate variability, in particular by the observed long-term trends in soil and air temperature. Longer vegetative and net carbon uptake seasons (almost 1 month longer since 1998) are likely to be caused by warming temperatures in late summer delaying the onset of senescence. A reduction in ecosystem respiration during the winter months is associated with lower temperatures in soil and air temperature during the same period. Each of these trends is responsible for about 50% of the total NEP increase at the MMSF for the past decade. Our results and conclusions leave open several questions, in particular those regarding the long-term duration of the observed trends, and the allocation of the 'extra' carbon uptake within the ecosystem components. These questions will be the focus of future research activities. However, our results confirm the great importance of long-term records in unraveling the mechanisms and feedbacks that regulate the interaction between ecosystems and climate variability, and therefore for the making of accurate predictions of the carbon dynamics in deciduous forest ecosystems.

Acknowledgements

Primary funding for this research was provided by the Office of Science (BER), US Department of Energy, through the Midwestern Center of the National Institute for Global Environmental Change (NIGEC), the National Institute for Climate Change Research (NICCR), and the Terrestrial Carbon Program (TCP). Any opinions, findings, and conclusions or recommendations expressed in this publication are those of the authors and do not necessarily reflect the views of the DOE. Access to the MMSF AmeriFlux site is provided by the Indiana Department of Natural Resources, Division of Forestry. The support and understanding of the MMSF Property Management is very much appreciated. We gratefully acknowledge the contributions of Scott Robeson (Indiana University) to the data analysis and interpretation, Steve Scott and the MMSF Field Crew to the operation and maintenance of the MMSF Flux Tower Facility.

References

Baldocchi DD (2008) Breathing of the terrestrial biosphere: lessons learned from a global network of carbon dioxide flux measurement systems. *Australian Journal of Botany*, **56**, 1–26.

Baldocchi DD, Black TA, Curtis PS *et al.* (2005) Predicting the onset of net carbon uptake by deciduous forests with soil temperature and climate data: a synthesis of FLUXNET data. *International Journal of Biometeorology*, **49**, 377–387.

Baldocchi DD, Falge E, Gu LH *et al.* (2001) FLUXNET: a new tool to study the temporal and spatial variability of ecosystem-scale carbon dioxide, water vapor, and energy flux densities. *Bulletin of the American Meteorological Society*, **82**, 2415–2434.

Black TA, Chen WJ, Barr AG *et al.* (2000) Increased carbon sequestration by a boreal deciduous forest in years with a warm spring. *Geophysical Research Letters*, **27**, 1271–1274.

Botta A, Viovy N, Ciais P, Friedlingstein P, Monfray P (2000) A global prognostic scheme of leaf onset using satellite data. *Global Change Biology*, **6**, 709–725.

Chmielewski FM, Rotzer T (2001) Response of tree phenology to climate change across Europe. *Agricultural and Forest Meteorology*, **108**, 101–112.

Churkina G, Schimel D, Braswell BH, Xiao XM (2005) Spatial analysis of growing season length control over net ecosystem exchange. *Global Change Biology*, **11**, 1777–1787.

Cramer W, Bondeau A, Woodward FI *et al*. (2001) Global response of terrestrial ecosystem structure and function to CO_2 and climate change: results from six dynamic global vegetation models. *Global Change Biology*, **7**, 357–373.

Crimmins MA, Crimmins TM (2008) Monitoring plant phenology using digital repeat photography. *Environmental Management*, **41**, 949–958.

Delpierre N, Dufrene E, Soudani K, Ulrich E, Cecchini S, Boe J, Francois C (2009) Modelling interannual and spatial variability of leaf senescence for three deciduous tree species in France. *Agricultural and Forest Meteorology*, **149**, 938–948.

Dragoni D, Caylor KK, Schmid HP (2009) Decoupling structural and environmental determinants of sap velocity Part II. Observational application. *Agricultural and Forest Meteorology*, **149**, 570–581.

Dragoni D, Schmid HP, Grimmond CSB, Loescher HW (2007) Uncertainty of annual net ecosystem productivity estimated using eddy covariance flux measurements. *Journal Of Geophysical Research-Atmospheres*, **112**, 1–9.

Dufrene E, Davi H, Francois C, Le Maire G, Le Dantec V, Granier A (2005) Modelling carbon and water cycles in a beech forest Part I: model description and uncertainty analysis on modelled NEE. *Ecological Modelling*, **185**, 407–436.

Ehman JL, Schmid HP, Grimmond CSB, Randolph JC, Hanson PJ, Wayson CA, Cropley FD (2002) An initial intercomparison of micrometeorological and ecological inventory estimates of carbon exchange in a mid-latitude deciduous forest. *Global Change Biology*, **8**, 575–589.

Estrella N, Menzel A (2006) Responses of leaf colouring in four deciduous tree species to climate and weather in Germany. *Climate Research*, **32**, 253–267.

Falge E, Baldocchi DD, Tenhunen J *et al*. (2002) Seasonality of ecosystem respiration and gross primary production as derived from FLUXNET measurements. *Agricultural and Forest Meteorology*, **113**, 53–74.

Gough CM, Flower CE, Vogel CS, Dragoni D, Curtis PS (2009) Whole-ecosystem labile carbon production in a north temperate deciduous forest. *Agricultural and Forest Meteorology*, **149**, 1531–1540.

Goulden ML, Munger JW, Fan SM, Daube BC, Wofsy SC (1996) Exchange of carbon dioxide by a deciduous forest: response to interannual climate variability. *Science*, **271**, 1576–1578.

Hollinger DY, Richardson AD (2005) Uncertainty in eddy covariance measurements and its application to physiological models. *Tree Physiology*, **25**, 873–885.

Hu J, Moore DJP, Burns SP, Monson RK (2010) Longer growing seasons lead to less carbon sequestration by a subalpine forest. *Global Change Biology*, **16**, 771–783.

Jonsson P, Eklundh L (2002) Seasonality extraction by function fitting to time-series of satellite sensor data. *IEEE Transactions on Geoscience and Remote Sensing*, **40**, 1824–1832.

Jonsson P, Eklundh L (2004) TIMESAT – a program for analyzing time-series of satellite sensor data. *Computers and Geosciences*, **30**, 833–845.

Keeling CD, Chin JFS, Whorf TP (1996) Increased activity of northern vegetation inferred from atmospheric CO_2 measurements. *Nature*, **382**, 146–149.

Leuning R (2004) Measurements of trace gas fluxes in the atmosphere using eddy covariance: WPL corrections revisited. In: *Handbook of Micrometeorology* (eds Lee X, Law B), pp. 119–132. Kluwer Academic, Dordrecht.

Linderholm HW (2006) Growing season changes in the last century. *Agricultural and Forest Meteorology*, **137**, 1–14.

Luyssaert S, Schulze ED, Borner A *et al*. (2008) Old-growth forests as global carbon sinks. *Nature*, **455**, 213–215.

Menzel A (2002) Phenology: its importance to the global change community – an editorial comment. *Climatic Change*, **54**, 379–385.

Menzel A, Fabian P (1999) Growing season extended in Europe. *Nature*, **397**, 659–659.

Menzel A, Sparks TH, Estrella N *et al*. (2006) European phenological response to climate change matches the warming pattern. *Global Change Biology*, **12**, 1969–1976.

Myneni RB, Keeling CD, Tucker CJ, Asrar G, Nemani RR (1997) Increased plant growth in the northern high latitudes from 1981 to 1991. *Nature*, **386**, 698–702.

Penuelas J, Rutishauser T, Filella I (2009) Phenology feedbacks on climate change. *Science*, **324**, 887–888.

Phillips RP, Bernhardt ES, Schlesinger WH (2009) Elevated CO_2 increases root exudation from loblolly pine (*Pinus taeda*) seedlings as an N-mediated response. *Tree Physiology*, **29**, 1513–1523.

Piao SL, Ciais P, Friedlingstein P *et al*. (2008) Net carbon dioxide losses of northern ecosystems in response to autumn warming. *Nature*, **451**, 49–53.

Piao SL, Friedlingstein P, Ciais P, Viovy N, Demarty J (2007) Growing season extension and its impact on terrestrial carbon cycle in the Northern Hemisphere over the past 2 decades. *Global Biogeochemical Cycles*, **21**, 1–11.

Press WH, Teukolsky SA, Vetterrling WT, Flannery BP (2002) *Numerical Recipes in C – The Art of Scientific Computing*. Cambridge University Press, Cambridge, UK.

Richardson AD, Bailey AS, Denny EG, Martin CW, O'keefe J (2006) Phenology of a northern hardwood forest canopy. *Global Change Biology*, **12**, 1174–1188.

Richardson AD, Black TA, Ciais P *et al*. (2010) Influence of spring and autumn phenological transitions on forest ecosystem productivity. *Philosophical Transactions of the Royal Society, Series B*, in press.

Richardson AD, Hollinger DY, Dail DB, Lee JT, Munger JW, O'keefe J (2009) Influence of spring phenology on seasonal and annual carbon balance in two contrasting New England forests. *Tree Physiology*, **29**, 321–331.

Richardson AD, Jenkins JP, Braswell BH, Hollinger DY, Ollinger SV, Smith ML (2007) Use of digital webcam images to track spring green-up in a deciduous broadleaf forest. *Oecologia*, **152**, 323–334.

Schimel DS, House JI, Hibbard KA *et al*. (2001) Recent patterns and mechanisms of carbon exchange by terrestrial ecosystems. *Nature*, **414**, 169–172.

Schmid HP, Grimmond CSB, Cropley F, Offerle B, Su HB (2000) Measurements of CO_2 and energy fluxes over a mixed hardwood forest in the mid-western United States. *Agricultural and Forest Meteorology*, **103**, 357–374.

Schmid HP, Su HB, Vogel CS, Curtis PS (2003) Ecosystem–atmosphere exchange of carbon dioxide over a mixed hardwood forest in northern lower Michigan. *Journal of Geophysical Research –Atmospheres*, **108**, 1–19.

Stöckli R, Rutishauser T, Dragoni D *et al*. (2008) Remote sensing data assimilation for a prognostic phenology model. *Journal of Geophysical Research – Biogeosciences*, **113**, 1–19.

Stöckli R, Vidale PL (2004) European plant phenology and climate as seen in a 20-year AVHRR land-surface parameter dataset. *International Journal of Remote Sensing*, **25**, 3303–3330.

Valentini R, Matteucci G, Dolman AJ *et al*. (2000) Respiration as the main determinant of carbon balance in European forests. *Nature*, **404**, 861–865.

Vitasse Y, Porte AJ, Kremer A, Michalet R, Delzon S (2009) Responses of canopy duration to temperature changes in four temperate tree species: relative contributions of spring and autumn leaf phenology. *Oecologia*, **161**, 187–198.

Wayson CA, Randolph JC, Hanson PJ, Grimmond CSB, Schmid HP (2006) Comparison of soil respiration methods in a mid-latitude deciduous forest. *Biogeochemistry*, **80**, 173–189.

White MA, De Beurs KM, Didan K *et al*. (2009) Intercomparison, interpretation, and assessment of spring phenology in North America estimated from remote sensing for 1982–2006. *Global Change Biology*, **15**, 2335–2359.

White MA, Nemani AR (2003) Canopy duration has little influence on annual carbon storage in the deciduous broad leaf forest. *Global Change Biology*, **9**, 967–972.

White MA, Running SW, Thornton PE (1999) The impact of growing-season length variability on carbon assimilation and evapotranspiration over 88 years in the eastern US deciduous forest. *International Journal of Biometeorology*, **42**, 139–145.

Willmott CJ, Matsuura K, Robeson SM (2009) Ambiguities inherent in sums-of-squares-based error statistics. *Atmospheric Environment*, **43**, 749–752.

Wofsy SC, Goulden ML, Munger JW *et al*. (1993) Net exchange of CO_2 in a midlatitude forest. *Science*, **260**, 1314–1317.

Yanling S, Hans WL, Deliang C, Alexander W (2010) Trends of the thermal growing season in China, 1951–2007. *International Journal of Climatology*, **30**, 33–43.

Yuan WP, Luo YQ, Richardson AD *et al*. (2009) Latitudinal patterns of magnitude and interannual variability in net ecosystem exchange regulated by biological and environmental variables. *Global Change Biology*, **15**, 2905–2920.